

---

## **Preparation and Characterization of a Surface Modified Amberlite IRA 402 Resin by Nano Iron Oxide and its Application for Uranium Separation**

Sadeek Sadeek<sup>a\*</sup>, Mohammed Galal<sup>b</sup>, Mohammed shiera<sup>c</sup>, Mahmoud Ramadan<sup>d</sup>,  
Mohammed Ramadan<sup>e</sup>

<sup>a</sup>Department of Chemistry, Faculty of Science, Zagazig University, Zagazig, Egypt

<sup>b,c,d,e</sup>Nuclear Material Authority

P.O. Box 530, Maadi Kattameya, Cairo, Egypt

### **Abstract**

A nano-iron oxide modified Amberlite IRA402 resin was prepared by the reaction of iron (II) and iron(III) ions in the presence of ammonium solution. The modified resin has been characterized by transmission electron microscopy, FTIR, X-ray diffraction, and scanning electron microscope images. In a batch experiments, uranium adsorption was evaluated using the modified Amberlite resin. The adsorption parameters studied were pH, contact time and the sorbent amount. The maximum adsorption capacity of the modified resin for uranium was 267.85 mg/g. Finally, modified Amberlite IRA-402 could be successfully used for separation of uranium from Sinai claystone leach liquor more than Amberlite IRA-402 without any modification.

**Keywords:** Uranium; Adsorption; Nano iron oxide; Modified Amberlite IRA402; Characterization.

---

\* Corresponding author.

## **1. Introduction**

Uranium is an important element in the development and utilization of nuclear power. A number of methods have been developed for the recovery of uranium, including extraction (solvent extraction, chromatographic extraction), precipitation (chemical precipitation, co-precipitation), exchange (ion exchange), flotation and adsorption, and each has its merits and limitation in the application [1-5]. Ion exchange and sorption are the most popular methods which have been widely practiced for uranium removal or recovery [6,7]. Uranium sorption on various natural sorbents and resins is important from economical and environmental viewpoints [8]. Numerous adsorbents such as Chitosan, activated sludges, organic biomass, zeolites, clays, metal oxides and carbons were developed for the adsorption of uranium [3, 9-13]. However, the separation process of adsorbents from aqueous solution is usually complex and time-consuming after saturated adsorption.

Nano materials are new solid materials that have attracted to solid phase extraction methods substantially due to their special and unique properties (such as high surface-volume ratios, high reactivities, etc.) [14,15]. Recently, magnetic nanoparticles as adsorption materials have been employed for removal of trace metals from water samples [16-18]. Magnetic nanoparticles are particularly attractive due to their unique properties such as excellent magnetic responsivity, high dispersibility, relatively large surface area and easiness of surface modification which enable them to have a wide range of potential applications in biological, environmental and food analysis [19,20]. The surface modification of resin with magnetic nanoparticles plays an important role in the selective preconcentration and separation of metals. The modification process occur through , a homogeneous distribution of inorganic nanomaterials on surface of the organic polymer leading to improve the interfacial interactions between them to give a new composite materials with improved performance for application and properties such as (physical and chemical properties, dielectric and mechanical properties, electrical conductivity, thermal stability, flame retardancy, and resistance to chemical reagents) compared with their individual constituents [21-23]. Nanoscale particles typically aggregate in the individual state, but give well dispersion through the modification process with the polymer matrix. The surface-functionalization of nanoscale particles is an essential step to form nanostructured hybrid composites. The lack of filler–matrix bonding or coupling often leads to the preparation of hybrid materials with nonisotropic properties and relatively poor mechanical behavior, which limits their application. Therefore, enhanced dispersion of nanofillers in the bulk of different organic matrices through surface modification is a challenge and technically required [24]. Moreover, the effects of wetting, permeability, fouling, and corrosion in the formed composite can be suppressed, or at least mitigated, by treating the surface of the inorganic filler. The high surface reactivity of most inorganic fillers facilitates their surface modification and functionalization. Selected metal oxide nanoscale particles, such as zinc oxide, titanium oxide, copper oxide, magnetite , and maghemite. Magnetic nanoparticle, particularly  $\text{Fe}_3\text{O}_4$  nanoparticle had gained increasing attention because of its unique magnetic properties and feasibility of preparation [25]. Because of the desirable properties and application of metal oxide/polymer hybrid nanocomposites, its synthesis has attracted increasing attention and many researchers have begun seeking new strategies for engineering nanocomposite materials.

In this study, the modified Ambelite IRA420 with nano iron was prepared and characterized. Consequently, the objective of this study is to assess the feasibility of using Ambelite IRA420 with iron nanoparticles for uranium

recovery, which can improve uranium extraction, and to optimize the factors to impact maximum extraction efficiency. The most important factors used are sample pH, the amount of the sorbent at a certain uranium concentration and contact time (min).

## **2. Experimental**

### **2.1 Instrumentation**

The surface morphology of Fe<sub>3</sub>O<sub>4</sub> and distribution of Fe<sub>3</sub>O<sub>4</sub> on the resin was performed in the ESEM LAB, Nuclear Materials Authority, Cairo, Egypt, using the Philips XL30 Environmental Scanning Electron Microscope (ESEM) attached with an energy dispersive X-ray analyzer (EDAX) unit. Transmission electron microscope (TEM) images were obtained using a JEOL JEM-2100 instrument using an accelerating voltage of 200 kV. Samples were ultra-sonicated in ethanol for 15 min and then dispersed on copper grids. Fourier transform infrared (FTIR) spectra were measured at room temperature in the wavenumber range (400–4,000 cm<sup>-1</sup>) on a Jasco FT/IR-6100. X-ray diffraction (XRD) was carried out with a Philips X-ray unit, Nuclear Materials Authority, Cairo, Egypt, model PW 223/20 operated at 40 kV and 20 mA. The UA-3 (Sintrex UA-3) uranium analyzer is used for the measurements of uranium in aqueous solutions.

The pH was measured using HANNA Instruments 8519 digital pH-meter. Calibrations of the electrode were carried out with standard buffer solutions, using pH values of both 7.00 and 4.01. The routine equipments used in this study were: drying oven (Qallenhamr), Analytical balance (Sartorous), magnetic stirrer and hot plate (IKA- Combimag ret.). Water distiller (Haeous) and equipments for classical extraction and measurements such as; burettes, conical flask, porcelain evaporating dishes, measuring spoon, filtration systems, desiccators and usual glass wares.

### **2.2 Chemicals and Reagents**

Analytical grade chemicals were used throughout this work. Sigma-Aldrich, USA was used for the preparation of nano iron. Amberlite IRA 402 were from Merck, USA. Stock solution of uranium (1000 ppm) was prepared by dissolving an accurately weighed amount of uranyl acetate (Fluka) in distilled water. Other working solutions of uranium were prepared by diluting the stock solution with distilled water.

### **2.3 Preparation of modified ion exchange**

The nano Fe<sub>3</sub>O<sub>4</sub> synthesis is based on reacting iron (II) and iron (III) ions in an aqueous ammonia solution to form magnetite, Fe<sub>3</sub>O<sub>4</sub>, as shown in eq (1).



This magnetite may be prepared in less than 2 h in an easy and economical method in which 1.0 ml of FeCl<sub>2</sub> solution and 4.0 ml of FeCl<sub>3</sub> solution was Combined. Place a magnetic stirring bar in the flask and begin stirring vigorously. Add dropwise by buret 50 ml of 0.7 M aqueous NH<sub>3</sub> solution into the flask. We

have found that the slow rate of addition is critical. Magnetite, a black precipitate, will form immediately. Stir throughout the addition of the ammonia solution. Cease stirring and allow the precipitate to settle (5–10 min). The formed Fe<sub>3</sub>O<sub>4</sub> washed several times using deionized water and then dried in an oven at 100° C over night.

The modified ion-exchange was carried out in situ by mixing 2g Amberlite IRA-402 resin with 4 mL of 1 M ferric chloride (1 M FeCl<sub>3</sub> in 2 M HCl) and 1 mL of 2 M ferrous chloride (2 M FeCl<sub>2</sub> in 2 M HCl) solution with stirring. Continuous stirring throughout the addition of 50 mL 1 M aqueous ammonia solution for 5 min was made. Excess reagent was removed by subsequent washing of the resin with deionized water. It was finally dried in an oven at about 100 C for 24 h forming a new sorbent.

## **2.5 Methods**

Fifty mg of the modified resin (MAIRA 402) were mixed with 50 ml of 750 ppm uranium solution acidified with sulfuric acid for 30 min. After solid-liquid separation, uranium was analyzed by the Sintrex UA-3 uranium analyzer. Each experiment was carried out three times and the average results were calculated. Extraction efficiency and the adsorption capacity of uranium on the sorbent surface were calculated using the following equations:

$$\text{Extraction, \%} = \frac{C_0 - C}{C_0} \times 100 \quad (2)$$

$$q \text{ (mg/g)} = \frac{(C_0 - C)V}{m} \quad (3)$$

Where C<sub>0</sub> and C are initial and final uranium concentration in solution, respectively, V is the volume of the uranium aqueous solution, m is the amount of the sorbent and q is the capacity of the sorbent.

## **3. Result and discussions**

### **3.1 Characterization of modified ion exchange**

Microphotograph of both AIRA402 and MAIRA402 are shown in figure 1A & B, respectively. The used Amberlite IRA-402 is anion exchange resin and has physical form of pale yellow translucent spherical beads as shown in Figure (1A), with particle size from 0.600–0.750 mm, its matrix is a styrene divinylbenzene copolymer and functional group of trimethyl ammonium. Figure 1B shows that the resin produced after modification is dark red. It was believed that the red color represents the formation of iron-resin bond.

#### **3.1.1 SEM analysis**

The SEM images of prepared nano-Fe<sub>3</sub>O<sub>4</sub> (AIRA402) and MAIRA402 samples are shown in Figures 2 and 3

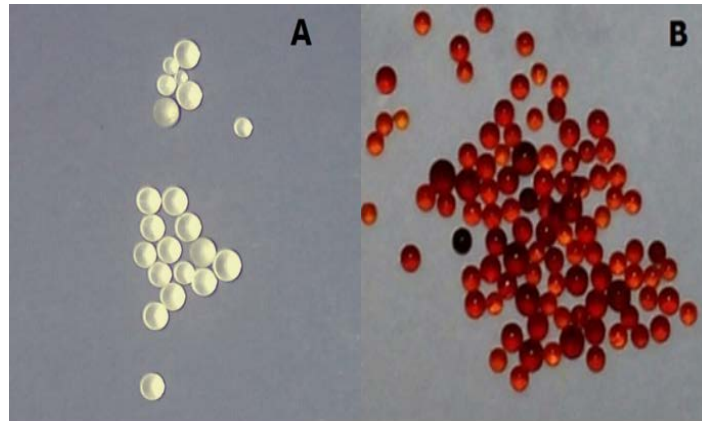


**Figure 1:** Microphotograph of AIRA402 (A) and MAIRA402 (B).



**Figure 2:** SEM images of prepared nano-Fe<sub>3</sub>O<sub>4</sub>.

The average size and shape of the synthesized magnetite nanoparticles were obtained using SEM (Figure 2). The surface morphology of the SEM image shows irregular shapes. In addition, we can find that Fe<sub>3</sub>O<sub>4</sub> nanoparticles appear to aggregate during the process of filtration and drying because of the large specific surface area (surface-to-volume ratio) and high surface energy. The surface of the AIRA402 was coated with the prepared nano-Fe<sub>3</sub>O<sub>4</sub> after the modification process.

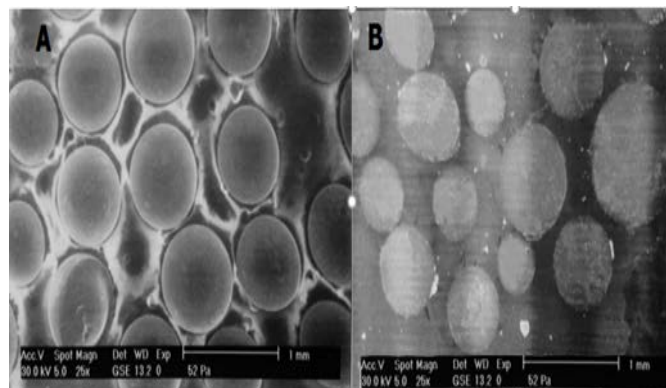


**Figure 3:** SEM micrograph of the AIRA402 (A), MAIRA402 (B)

### 3.3.2 TEM analysis

TEM analysis of the prepared nano-Fe<sub>3</sub>O<sub>4</sub> and digital diffraction pattern of MAIRA402 was shown in Figure 4A & B, respectively.

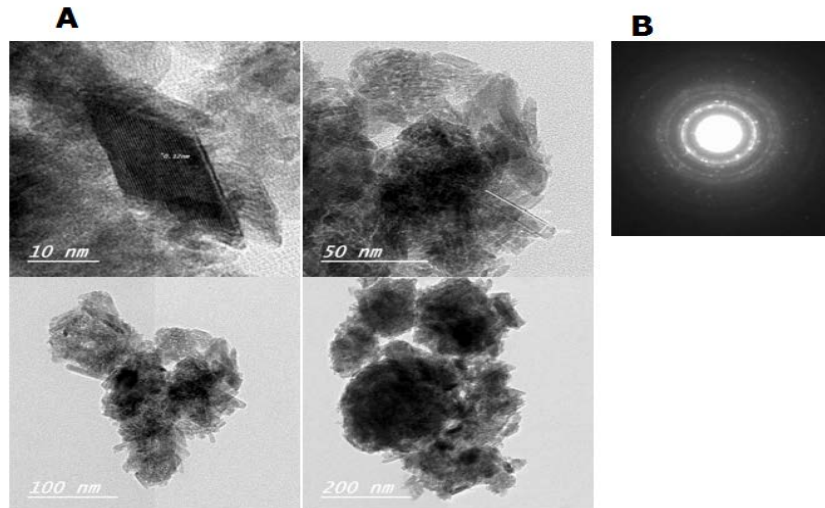


**Figure 4:** TEM images of nano magnetic Fe<sub>3</sub>O<sub>4</sub> nanoparticles (A) and digital diffraction pattern of MAIRA402 (B)

The TEM images (Figure 4A) show that Fe<sub>3</sub>O<sub>4</sub> nanoparticles are highly agglomerated into clusters, probably due to the drying and filtration process. As well as, the high surface area and magnetic dipole–dipole interactions between particles. The TEM diffraction ring (Figure 4B) shows that the Fe<sub>3</sub>O<sub>4</sub> nanoparticles exhibit a crystalline state after modification with AIRA402.

### 3.1.3 FTIR analysis

FTIR used to identify the modification with Fe<sub>3</sub>O<sub>4</sub>. The IR spectra of nano Fe<sub>3</sub>O<sub>4</sub> and MAIRA402 were compared and shown in figure (5).

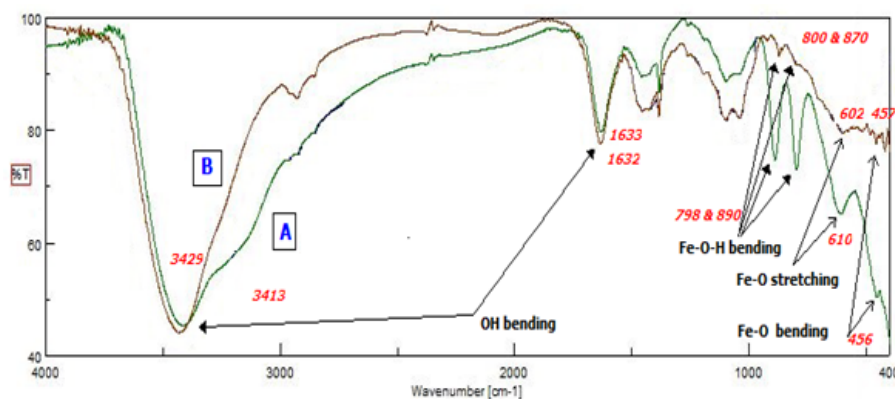


**Figure 5:** FTIR spectra of the prepared nano Fe<sub>3</sub>O<sub>4</sub> (A) and MAIRA402 (B)

The FTIR spectra (5A) shows several absorption bands at 3413, 1632, 890, 798, 610, and 456  $\text{cm}^{-1}$ . The characteristic peaks of  $\text{Fe}_3\text{O}_4$  occurs at 456 and 610  $\text{cm}^{-1}$  which attributed to the bending and stretching vibration of the Fe-O bond, respectively (Figure 5A). The  $\text{Fe}_3\text{O}_4$  peaks appeared in the same regions with a noticeable slight shift in spectrum B at 457, 602  $\text{cm}^{-1}$  (Figure 5B). The slight shifts in normal stretching and bending modes of the Fe-O bonds suggest that nano- $\text{Fe}_3\text{O}_4$  particles are homogeneously distributed throughout the surface of Amberlite IRA 402 as a composite material.

The characteristic peaks that occurs at 798 and 890  $\text{cm}^{-1}$  which can be assigned to Fe-O-H bending vibrations, changed to a bands of very weak intensity at 800 and 870  $\text{cm}^{-1}$ , confirming the presence of a small amount of  $\alpha$ -FeOOH in the prepared MAIRA402 sample.

The band at 1632  $\text{cm}^{-1}$  is usually attributed to the OH bending vibrations and the broadest band at 3413  $\text{cm}^{-1}$  should be attributed to the OH stretching vibration combined with Fe atoms. The FT-IR results suggest the presence of bound water in the  $\text{Fe}_3\text{O}_4$  structure. The OH peaks appeared in the same regions with a slight shift in spectrum B at 1633 and 3429  $\text{cm}^{-1}$ . It is concluded that the  $\text{Fe}_3\text{O}_4$  nanoparticles is successfully bound to the surface of resin.

### 3.1.4 XRD analysis

The XRD pattern for prepared nano  $\text{Fe}_3\text{O}_4$  and MAIRA402 samples are shown in Figure 6A & B respectively.

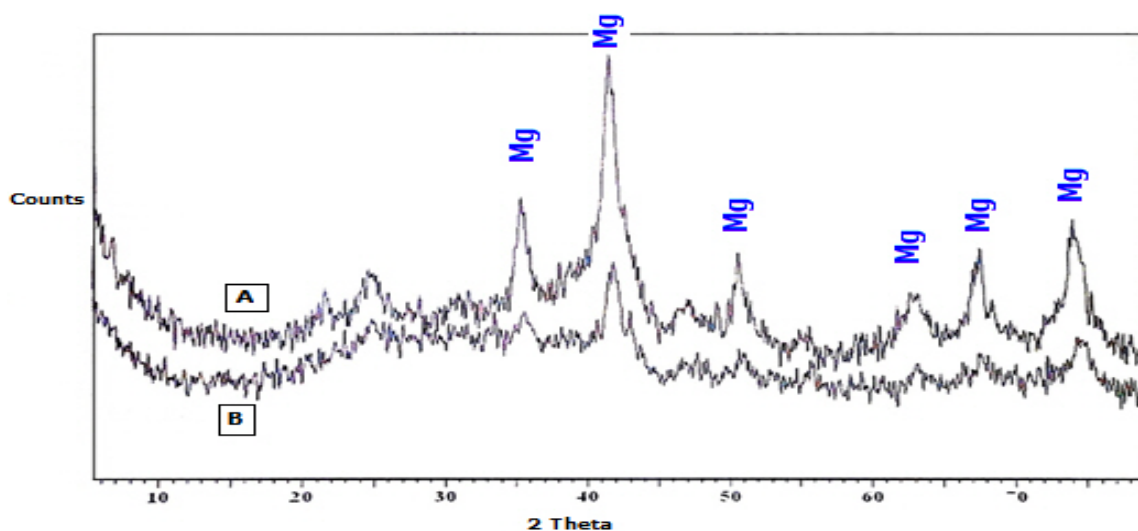


**Figure 6:** X-ray diffraction pattern for (a) prepared nano  $\text{Fe}_3\text{O}_4$  sample (b) MAIRA402 sample

As shown in Figure (6A), six characteristic peaks for nano  $\text{Fe}_3\text{O}_4$  (Mg),  $2\theta = 35.325, 41.650, 50.825, 63.270, 68.015$  and  $74.675$  was identified, These peaks are agree with the database of standard magnetite iron oxide of (ASTM Card No: 86-1359).

Figure (6b) represents the XRD pattern of MAIRA402 sample showing the characteristics peaks of  $\text{Fe}_3\text{O}_4$  which are slightly shifted to  $35.392, 41.690, 50.90, 63.281, 68.025$  and  $74.689$  with very weak intensities

resulting from the formation of MAIRA402 and clarifying the stability of the crystalline phase of Fe<sub>3</sub>O<sub>4</sub> nanoparticle after the modification with Amberlite IRA-402. It was also concluded that nano Fe<sub>3</sub>O<sub>4</sub> was successfully immobilized on the surface of Amberlite IRA-402.

### **3.2 Uranium recovery experiments**

#### **3.2.1 Standard uranium solution**

A standard uranium solution of 1000 ppm was prepared by dissolving 1.78 g of uranyl acetate in (1L) double distilled water. Sulfuric acid was added to enhance the formation of uranyl sulfate complexes such as UO<sub>2</sub>(SO<sub>4</sub>)<sub>2</sub><sup>2-</sup> and UO<sub>2</sub>(SO<sub>4</sub>)<sub>3</sub><sup>4-</sup>. Different factors have been carefully applied in order to obtain the optimum extraction of uranium into the studied resin (MAIRA402). These factors include pH, time, and the amount of the sorbent at a certain U concentration. To study the effect of these factors on uranium extraction, different series of experiments have been performed.

##### **3.2.1.1 Effect of pH**

The pH has a great effect on the uranium adsorption through MAIRA402 in aqueous solution and the binding sites located at the adsorbents surface. The pH was varied from 3 to 4, to discover the optimum pH for the sorption of uranium on the MAIRA402, while the other parameters were kept constant. We should keep the pH at this range because at pH below 3, the extraction efficiency decreased as magnetite nanoparticles soluble in acidic solutions. Increasing the pH more than 4, the uranium starts to precipitate, until all uranium precipitate at pH=7.5. Also at pH more than 6, the binding ability of the sorbent to the uranyl ions will decrease, because of the strong basic medium affect on the bending sites on surface of the sorbent leading to decrease the extraction efficiency.

Fifty ml of 750 ppm standard uranium solution (contain 37.5mg), the time of agitation 30 minutes, at room temperature, and 0.05g (50mg) of MAIRA402. The results were shown in Table (1)

**Table 1:** Effect of pH upon uranium extraction

PH	3.3	3.6	3.9	4.2
U, extraction, %	28	31	38	37

From the results given above, it is clear that the recovery percent of uranium ions was increased by increasing pH to give a greater value at 3.9. Uranium adsorption capacity (q) of 14.25 mg was obtained.

##### **3.2.1.2 Effect of agitation time**

The effect of agitation time on uranium adsorption was studied at the interval (10 – 100 minutes) while the other factors were kept constant at 50ml of 750 ppm standard uranium solution, pH 3.9, at room temperature and 0.05g of MAIRA402. The steering process should be slow, therefore, don't affect the resin cohesion. The

obtained results are tabulated in Table (2)

**Table 2:** Effect of time upon uranium extraction

Time, minutes	10	20	30	40	50	60	70	80	90
U, extraction, %	20	29	38	45	52	60	71	79	79

The obtained data summarizes the results from the adsorption of uranium at different time, by increasing the time the adsorption increase until reached to the saturation point in 80 min of uranium adsorption capacity ( $q$ ) 29.62 mg was obtained. After that, no significant change in the adsorption of uranium was obtained.

### 3.2.1.3 Effect of the sorbent amount

The effect of sorbent amount on uranium adsorption was studied by taken different amounts of sorbent (0.03-0.15g), while the other factors were kept constant at 50ml of 750 ppm standard uranium solution, the time of agitation 80 minutes, pH 3.9, at room temperature and 0.05g of MAIRA402. The obtained results are tabulated in Table (3)

**Table 3:** Effect of sorbent amount upon uranium extraction

The sorbent amount	0.03	0.05	0.07	0.09	0.12	0.13	0.14	0.15
U extraction, %	74	79	83.5	88	95	97.5	100	100

From the results given above, it is clear that the recovery percent of uranium ions was increased by increasing the sorbent amount until all uranium (37.5 mg) had been completely adsorbed on 0.14 g MAIRA402, and any excess of the sorbent amount doesn't change in uranium extraction efficiency, but leads to more unsaturated sites on the new sorbent.

Finally, 500 ml of 750 ppm uranium at the optimum conditions (pH= 3.9, agitation time 80 minutes, at room temperature), the all uranium amount was successfully adsorbed on the 1.4 g of MAIRA402 with a maximum adsorption capacity ( $q_{\max}$ ) = 267.85 mg/g of MAIRA402 that compared with only 206 mg/g for AIRA402 without any modification at the same experimental conditions.

### 3.2.2 Sinai leach liquor

A typical leach solution from the claystone leaching test contains 600, 700 ppm of total iron and uranium respectively was prepared. Oxidation by  $H_2O_2$  followed by precipitation at pH 4 has been proposed to minimize the harmful effects of interfering ions such as iron and alumina oxide upon the resin, since resin has higher affinity toward the interfering ions than uranium.

The uranium absorption optimum condition (pH=3.9, agitation time 80 minutes and at room temperature) with a maximum adsorption capacity  $q_{\max}$  = 267.85 mg/g of MAIRA402 has been applied to claystone leach liquor,

92.5 % uranium extraction was obtained. This indicates that MAIRA402 would likely be feasible for absorption of uranium from claystone in the presence of iron and alumina.

#### **4. Conclusions**

The modification process occurs through; a homogeneous distribution of inorganic nano-magnetite with the organic polymer leading to improve the interfacial interactions between them to give a new composite materials with improved performance for application and properties, the new composite was characterized by transmission electron microscopy, FTIR, X-ray diffraction, and scanning electron microscope images. In a batch experiments, uranium adsorption was successfully with the maximum capacity of the modified Amberlite resin 267.85 mg/g, The adsorption parameters studied were pH, contact time and the sorbent amount Finally, modified Amberlite IRA-402 could be successfully used for separation of uranium from Sinai claystone leach liquor.

#### **References**

- [1] A. Mellah, S. Chegrouche and M. Barkat (2005) The removal of uranium( VI) from aqueous solutions onto activated carbon: kinetic and thermodynamic investigations. *J Colloid Interface Sci* 296:434–441.
- [2] J.L. Lapka, A. Paulenova, M.Y. Alyapyshev, V.A. Babain, R.S. Herbst, and J.D. Law (2009) Extraction of uranium(VI) with diamides of dipicolinic acid from nitric acid solutions. *Radiochim Acta* 97:291–296.
- [3] Xie SB, Zhang C, Zhou XH, Yang J, Zhang XJ, Wang JS (2009) Removal of uranium(VI) from aqueous solution by adsorption of hematite. *J Environ Radioact* 100:162–166.
- [4] T.S. Anirudhan, C.D. Bringle and S. Rijith (2010) Removal of uranium (VI) from aqueous solutions and nuclear industry effluents using humic acid-immobilized zirconium-pillared clay. *J Environ Radioact* 101:267–276.
- [5] A. Rout, K.A. Venkatesan, T.G. Srinivasan and P.R. Vasudeva (2012) Liquid–liquid extraction of Pu(IV), U(VI) and Am(III) using malonamide in room temperature ionic liquid as diluent. *J Hazard Mater* 221–222:62–67
- [6] A. Kilislioglu and B.Bilgin (2002) Adsorption of uranium on halloysite, *Radiochim. Acta* 90:155-160
- [7] S.H. Choi, M.S. Choi, Y.T. Park, K.P. Lee and H.D. Kang (2003) Adsorption of uranium ions by resins with amidoxime and amidoxime/carboxyl group prepared by radiation-induced polymerization, *Radiat. Phys. Chem.* 67:387-390
- [8] R. j. Qadeer, M. Hanif, and M. Saleem, Uptake of uranium ions by molecular sieve, *Radiochim. Acta* 68(1995)197-201.

- [9] S.H. Hasan, P. Srivastava and M. Talat (2010) Bioadsorption of lead using immobilized *Aeromonas hydrophila* biomass in up flow column system: factorial design for process optimization. *J Hazard Mater* 177:312–322.
- [10] H. Hu, Z. Wang, L. Pan (2010) Synthesis of monodisperse  $\text{Fe}_3\text{O}_4$  coated silica microspheres and their application for removal of heavy metal ions from water. *J Alloy Compd* 492:656–661.
- [11] T.S. Anirudhan and S. Rijith (2012) Synthesis and characterization of carboxyl terminated poly(methacrylic acid) grafted chitosan/ bentonite composite and its application for the recovery of uranium(VI) from aqueous media. *J Environ Radioact* 106:8–19.
- [12] F.S. Gomes, Dina L. Lopez and Ladeira Cláudia Q (2012) Characterization and assessment of chemical modifications of metal-bearing sludges arising from unsuitable disposal. *J Hazard Mater* 199–200:418–425.
- [13] L.M. Zhou, C. Shang, Z.R. Liu, G.L.Huang, and A.A. Adesoji (2012) Selective adsorption of uranium(VI) from aqueous solutions using the ion-imprinted magnetic chitosan resins. *J Colloid Interface Sci.* 365:165–172.
- [14] N. Tran and T.J. Webster (2010) Magnetic nanoparticles: biomedical applications and challenges. *J Mat Chem* 20:8760–8767.
- [15] A. Henglein (1989) Small-particle research: physicochemical properties of extremely small colloidal metal and semiconductor particles, *Chem. Rev.* 89:1861–1873.
- [16] A.F. Ngomsik, A.Bee, M.Draye, G. Cote and V. Cabuil (2005) Magnetic nano- and microparticles for metal removal and environmental applications: a review, *C.R. Chimie* 8:963–970.
- [17] W. Yantasee, C.L Warner, T. Sangvanich, R.S. Addleman, T.G. Carter, R.J. Wiacek, G.E. Fryxell, C. Timchalk, and M.G. Warner (2007) Removal of heavy metals from aqueous systems with thiol functionalized superparamagnetic nanoparticles, *Environ Sci. Technol.* 41 5114–5119.
- [18] S. Sadeghia, H. Azhdaria, H. Arabib and Z. A. Moghaddama (2012): Surface modified magnetic  $\text{Fe}_3\text{O}_4$  nanoparticles as a selective sorbent for solid phase extraction of uranyl ions from water samples, *Journal of Hazardous Materials*, 215– 216, 208– 216.
- [19] J.S. Suleiman, B. Hu, H. Peng and C. Huang (2009) Separation/preconcentration of trace amounts of Cr, Cu and Pb in environmental samples by magnetic solid-phase extraction with Bismuthiol-II-immobilized magnetic nanoparticles and their determination by ICP-OES, *Talanta* 77 :1579–1583.
- [20] A. A. Elabd, M.M Abo-aly, W. I. Zidan, E. Bakier and M. S. Attia (2012): Modified Amberlite

- (IR120) by magnetic nano iron-oxide for uranium removal, *Analytical Chemistry Letters*, 3(1), 46-64.
- [21] V. K. Thakur and M. K. Thakur (2014). Processing and characterization of natural cellulose fibers/thermoset polymer composites. *Carbohydrate polymers*, 109, 102-117.
- [22] S. Kalia, S. Boufi, A. Celli and S. Kango (2014) Nanofibrillated cellulose: surface modification and potential applications. *Colloid and Polymer Science*, 292(1), 5-31.
- [23] S. Kalia, B. S. Kaith, and I. Kaur (Eds.) (2011) *Cellulose fibers: bio-and nano-polymer composites: green chemistry and technology*. Springer Science & Business Media.
- [24] M. Z. Rong, M. Q. Zhang and W. H. Ruan (2006). Surface modification of nanoscale fillers for improving properties of polymer nanocomposites: a review. *Materials science and technology*, 22(7), 787-796.
- [25] F.L. Fan, Z. Qin, J. Bai, W.D. Rong, F.Y. Fan, W. Tian, X.L. Wu, Y. Wang and L. Zhao (2012) Rapid removal of uranium from aqueous solutions using magnetic  $\text{Fe}_3\text{O}_4@\text{SiO}_2$  composite particles. *J Environ Radioact* 106:40–46.